Inorganic Chemistry

Communication

pubs.acs.org/IC

Synthesis, Lattice Dynamics, and Mechanical Properties of a High-Pressure Scheelite Phase of RVO_4

Zuocai Huang,[†] Lei Zhang,[†] and Wei Pan*,[†]

[†]State Key Laboratory of New Ceramics and Fine Processing, Department of Materials Science and Engineering, Tsinghua University, Beijing 100084, China

Supporting Information

ABSTRACT: High-pressure scheelite phases of RVO_4 (R = Y, Sm, Gd, Yb, Lu) compounds were prepared by high pressure (up to 25 GPa) from zircon RVO_4 compounds. Raman spectra of these scheelite phases of RVO_4 were determined and discussed in detail. Mechanical properties, including bulk, shear, Young's modulus, B/G and Poisson's ratios, of the scheelite phase of RVO_4 were measured by an ultrasonic method and compared with the results calculated by density functional theory. The calculated lattice parameters and mechanical properties are in good agreement with the experimental results. The radius and states of the 4f orbital of R show distinct effects on the mechanical properties.

Compounds of the family RVO_4 (R = rare-earth elements, Sc, Y) have been widely used as promising optical materials for birefringent solid-state laser applications.[1,2] What is more, RVO_4 compounds are also used as cathodoluminescent materials, thermophosphors, photocatalysis materials, and in lithium-ion batteries.[3−6] RVO_4 compounds crystallize in a zircon structure (space group $I4_1/amd$ and $Z = 4$) at ambient conditions, and they transform upon moderate pressure to a denser scheelite-type phase (space group $I4_1/a$ and $Z = 4$) like ABO_4 compounds such as $ZrSiO_4$.[7] The phenomenon of the phase transition from zircon to scheelite has attracted much interest.[8−11] Syassen et al.[8] studied the phase transition process of YVO_4, and they found that zircon-type YVO_4 transforms to a scheelite-type structure upon 8.5 GPa and zircon YVO_4 transforms into scheelite YVO_4 completely at 16 GPa. Errandonea et al.[9] studied several zircon-type orthovanadates such as $ScVO_4$, $LuVO_4$, and $EuVO_4$ by X-ray diffraction, and the relationship between the lattice parameters and pressure of these compounds was also discovered. Ding et al.[10] studied the phase transition and the effect on the luminescence property of $GdVO_4$:Eu^{3+}. Errandonea et al.[11] studied the lattice dynamics of $ScVO_4$ upon different pressures by an in situ Raman investigation and density functional theory (DFT) calculation. However, it is very difficult to get pure scheelite RVO_4 because the complete phase transition pressure is too high, so there are few reports on the lattice dynamics and mechanical properties of high-pressure scheelite-type RVO_4. In this Communication, the pure scheelite RVO_4 were prepared via a high-pressure route (up to 25 GPa), using zircon RVO_4 as the precursor. The lattice dynamics and mechanical properties of high-pressure scheelite-type RVO_4 compounds were determined by experiments and calculations.

The zircon RVO_4 (R = Y, Sm, Gd, Yb, Lu) were prepared by a solid-state reaction method.[12] The samples were pressed up to 25 GPa for 2 h and then released to ambient conditions. The phase determination was carried out with X-ray diffraction, and the patterns (Figure 1) show that the compounds are pure

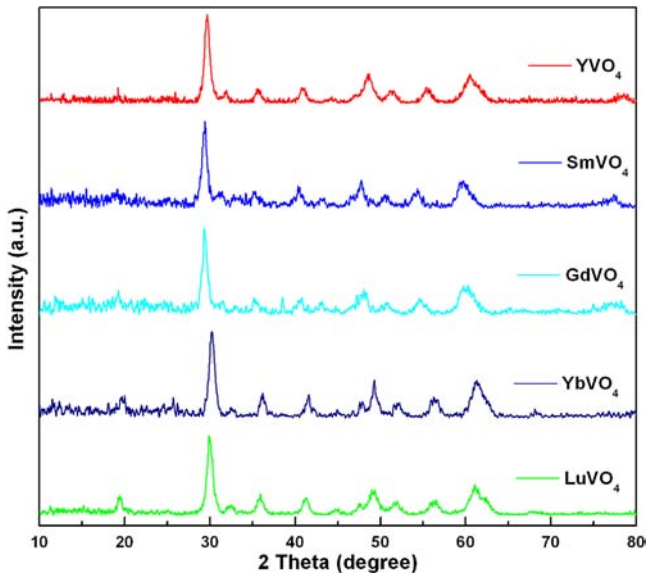

Figure 1. X-ray patterns of the scheelite phase of RVO_4 (R = Y, Sm, Gd, Yb, Lu).

scheelite structures. The lattice dynamics were determined by Raman spectroscopy, and mechanical properties were determined by an ultrasonic method.

First-principles calculation based on DFT[13] implemented through the *CASTEP* program[14] was employed to determine the mechanical properties. The local spin density approximation with additional Hubbard correlation terms (LSDA+U) was used as the exchange and correlation energy.

The lattice parameters of scheelite RVO_4 were determined by X-ray diffraction, and the values are shown in Table 1. The calculated parameters are also shown in Table 1 as a comparison. Only two kinds of scheelite RVO_4 (YVO_4[8] and $LuVO_4$[9]) have been investigated on their lattice parameters

Received: August 14, 2012
Published: October 17, 2012

dx.doi.org/10.1021/ic3017672 | *Inorg. Chem.* 2012, 51, 11235−11237

Table 1. Lattice Parameters (a and c) and Mechanical Properties of Scheelite RVO_4 (R = Y, Sm, Gd, Yb, Lu) Compounds

material	method	a	c	C_{11}	C_{33}	C_{44}	C_{66}	C_{12}	C_{13}	C_{16}	B	G	v	E	B/G
YVO_4 (r =1.02 Å)	GGA	5.06	11.30	233	193	54	69	109	89	−21	136	60	0.31	157	2.3
	LDA	4.96	10.99	271	245	64	80	139	117	−28	170	69	0.32	182	2.5
	LSDA+U	4.99	11.04	257	225	61	73	128	110	−26	159	65	0.32	171	2.5
	exp.[a]	5.03	11.25								140	60	0.31	158	2.3
	exp.[b]	5.03	11.23												
$SmVO_4$ (r =1.08 Å)	LSDA+U	5.09	11.36	192	187	57	96	77	92	−56	121	61	0.29	157	2
	exp.[a]	5.11	11.41								120	59	0.29	152	2
$GdVO_4$ (r =1.05 Å)	LSDA+U	5.02	11.05	279	251	79	85	146	129	−22	179	75	0.32	198	2.4
	exp.[a]	5.12	11.20								140	68	0.29	175	2.1
$YbVO_4$ (r =0.99 Å)	LSDA+U	4.96	10.88	243	172	55	41	125	79	−34	132	54	0.32	143	2.4
	exp.[a]	5.02	10.98								137	57	0.32	150	2.4
$LuVO_4$ (r =0.98 Å)	LSDA+U	4.98	11.06	290	277	65	76	154	138	−31	190	70	0.34	186	2.7
	exp.[a]	5.02	11.09								158	64	0.32	170	2.5
	exp.[c]	5.00	11.08												

[a]Experiment in this work. [b]Reference 9. [c]Reference 10. B represents the bulk modulus, G the shear modulus, E Young's modulus, v the Poisson ratio, and r radius of R.

formerly, and our experimental results are in good agreement with them. We also calculated the equilibrium lattice constants, and the optimized lattice parameters are in accordance with the experimental results. It is well-known that LSDA+U calculations usually underestimate the lattice constants, so the calculated results here are slightly smaller than the experimental results.

The space group symmetry of scheelite is $I4_1/a$ (point group C_{4h}^6). There are 12 atoms in the primitive cell, and there are 13 first-order Raman modes at the Brillouin zone center with symmetries $\Gamma = 3A_g + 5B_g + 5E_g$[15] in the Raman spectra. These modes can be further classified as either internal (ν_1 to ν_4) or external (T and R) modes of the VO_4 units.

$$\Gamma = \nu_1(A_g) + \nu_2(A_g) + \nu_2(B_g) + \nu_3(B_g) + \nu_3(E_g) + \nu_4(B_g) + \nu_4(E_g) + R(A_g) + R(E_g) + 2T(B_g) + 2T(E_g)$$

Raman spectra of scheelite RVO_4 are shown in Figure S2 in the Supporting Information (SI). From Figure S2 in the SI, it is seen that scheelite RVO_4 compounds show similar Raman characteristics and different modes. The Raman frequency and mode assignment of scheelite RVO_4 are shown in Table 2. The highest-frequency mode at about 830 cm^{-1} is assigned to the symmetric stretching mode $\nu_1(A_g)$, and its frequency is similar to the reported data.[11,16] The other two asymmetric stretching modes of scheelite RVO_4 were observed at about 810 and 750 cm^{-1} and assigned to $\nu_3(B_g)$ and $\nu_3(E_g)$. The four bending vibrations are observed at about 435, 415, 365, and 350 cm^{-1} and assigned to $\nu_2(A_g)$, $\nu_2(B_g)$, $\nu_4(B_g)$, and $\nu_4(E_g)$ modes. The other six external modes are also observed and assigned to external translational and rotational modes.

Table 2. Raman Frequency and Mode Assignment of Scheelite RVO_4 (R = Y, Sm, Gd, Yb, Lu) Compounds at Ambient Conditions

mode	$SmVO_4$	$GdVO_4$	YVO_4	$YbVO_4$	$LuVO_4$
$T(E_g)$	148	147	148	148	149
$T(B_g)$	180	176	165	165	163
$T(B_g)$	194	188	194	189	183
$T(E_g)$	201	200	201	200	209
$R(A_g)$	245	244	242	240	239
$R(E_g)$	321	321	320	318	318
$\nu_2(A_g)$	346	350	347	350	349
$\nu_2(B_g)$	368	368	369	365	368
$\nu_4(B_g)$	418	417	415	415	414
$\nu_4(E_g)$	435	435	437	434	432
$\nu_3(E_g)$	749	748	751	749	751
$\nu_3(B_g)$	811	809	811	808	806
$\nu_1(A_g)$	832	831	829	829	829

We also analyzed the electronic structure of scheelite RVO_4 shown in Figure S3 in the SI. Here, we just discuss the electronic structure of scheelite $GdVO_4$ (Figure S3c in the SI). The electronic structure of scheelite $GdVO_4$ is very similar to that of zircon $GdVO_4$ in our previous work.[12] The band gap calculated here is 2.94 eV, which is larger than zircon $GdVO_4$.[12] The spin-dependent density of states (DOS) is also shown in Figure S3c in the SI. The energy ranges of the DOS are mainly divided into three parts. Because the lower energy part has little effect on the electronic property, we just discuss the valence and conduction bands. The valence bands are mainly composed of O 2p states, hybridized with V 3d and Gd 4f states. The conduction bands are mainly composed of V 3d and Gd 4f states. The results of the Mulliken population indicate that two types of chemical bonds exist in RVO_4, that is, R−O and V−O bonds. It is found that there are two kinds of R−O bonds, which means that the dodecahedral structure is slightly distorted. The calculated overlap populations indicate that the V−O bonds possess larger bond order than the R−O bonds. The V−O bonds in RVO_4 are mainly covalent, while the R−O bonds are a mixture of covalent and ionic characteristics.

The mechanical properties from calculations and experiments are shown in Table 1. The theoretical elastic constants were calculated using a stress−strain method, and the mechanical properties of scheelite RVO_4 polycrystalline are evaluated from elastic constants within the Voigt−Reuss−Hill (VRH) approximation.[17] From Table 1, the mechanical properties calculated from LSDA+U are in accordance with the experimental results. For RVO_4 compounds, the radius of R has a great effect on the lattice parameters and mechanical properties. The smaller the radius of R is, the smaller the lattice parameters are, while the larger the elastic constants are. So, $LuVO_4$ has the largest elastic constants among the compounds studied. Besides the effects of R's radius, the 4f orbital also

dx.doi.org/10.1021/ic3017672 | Inorg. Chem. 2012, 51, 11235−11237

shows effects on the properties of RVO_4. For scheelite $GdVO_4$, Gd^{3+} shows a half-filled-shell 4f orbital; this reveals high stability and the fact that its mechanical properties are beyond the rule that the mechanical properties increase with a decrease of *R*'s radius.

The *B*/*G* value and Poisson's ratio (marked by *v*) of scheelite RVO_4 compounds are also shown in Table 1. From Table 1, the *B*/*G* values for RVO_4 compounds are all larger than 2.0 and their Poisson ratios are in the range of 0.29−0.33, so the scheelite RVO_4 compounds show ductile character, according to Pugh's criterion.[18] From Table 1, we can also find that the *B*/*G* value and Poisson's ratio are also affected by the radius of *R*.

In summary, the high-pressure scheelite RVO_4 compounds were prepared by high pressure (up to 25 GPa) from zircon RVO_4 compounds. The lattice parameters from experiments and calculations are in accordance with each other, and some results are reported for the first time and can be used as references for further investigations. Raman spectra of scheelite RVO_4 are analyzed in detail. The mechanical properties of scheelite RVO_4 were measured by ultrasonic methods and calculated by DFT. The calculated results are in good agreement with the experimental results. The radius and 4f orbital of *R* shows great effects on the mechanical properties of the sheelite RVO_4 compounds.

■ ASSOCIATED CONTENT

Supporting Information

Detailed experimental process, SEM, Raman spectra, and band structure and DOS of the samples RVO_4. This material is available free of charge via the Internet at http://pubs.acs.org.

■ AUTHOR INFORMATION

Corresponding Author

*E-mail: panw@mail.tsinghua.edu.cn.

Notes

The authors declare no competing financial interest.

■ ACKNOWLEDGMENTS

This research is supported by the National Science Foundation of China (Grant 50990302).

■ REFERENCES

(1) Ryba-Romanowski, W. *Cryst. Res. Technol.* **2003**, *38*, 225−236.
(2) Miyazawa, S. *Opto-Electron. Rev.* **2003**, *11*, 77−84.
(3) Shafi, S. P.; Kotyk, M. W.; Cranswick, L. M. D.; Michaelis, V. K.; Kroeker, S.; Bieringer, M. *Inorg. Chem.* **2009**, *48*, 10553−10559.
(4) Mullica, D. F.; Sappenifield, E. L.; Abraham, M. M.; Chakoumakos, B. C.; Boatner, L. A. *Inorg. Chim. Acta* **1996**, *248*, 85−89.
(5) Oshikiri, M.; Boero, M.; Matsushita, A.; Ye, J. H. *J. Chem. Phys.* **2009**, *131*, 034701−034708.
(6) Boatner, L. A.; Abraham, M. M.; Sales, B. C. *Inorg. Chim. Acta* **1984**, *94*, 146−150.
(7) Flórez, M.; Contreras-García, J.; Recio, J. M.; Marqués, M. *Phys. Rev. B* **2009**, *79*, 104101−104111.
(8) Wang, X.; Loa, I.; Syassen, K.; Hanfland, M.; Ferrand, B. *Phys. Rev. B* **2004**, *70*, 064109−064114.
(9) Errandonea, D.; Lacomba-Perales, R.; Ruiz-Fuertes, J.; Segura, A.; Achary, S. N.; Tyagi, A. K. *Phys. Rev. B* **2009**, *79*, 184104−184112.
(10) Zhang, C. C.; Zhang, Z. M.; Dai, R. C.; Wang, Z. P.; Zhang, J. W.; Ding, Z. J. *J. Phys. Chem. C* **2010**, *114*, 18279−18282.
(11) Panchal, V.; Manjon, F. J.; Errandonea, D.; Rodriguez-Hernandez, P.; López-Solano, J. *Phys. Rev. B* **2011**, *83*, 064111−064120.
(12) Huang, Z. C.; Zhang, L.; Feng, J.; Cui, X. J.; Pan, W. *J. Alloys Compd.* **2012**, *538*, 56−61.
(13) Hohenberg, P.; Kohn, W. *Phys. Rev. B* **1964**, *136*, 864−871.
(14) Segall, M. D.; Lindan, P. J. D.; Probert, M. J.; Pickard, C. J.; Harsnip, P. J.; Clark, S. J.; Panye, M. C. *J. Phys.: Condens. Matter* **2002**, *14*, 2717−2744.
(15) Rousseau, D. L.; Baumann, R. P.; Porto, S. P. *J. Raman Spectrosc.* **1981**, *10*, 253−290.
(16) Rao, R.; Garg, A. B.; Sakuntala, T.; Achary, S. N.; Tyagi, A. K. *J. Solid State Chem.* **2009**, *182*, 1879−1883.
(17) Chung, D. H.; Buessem, W. R. *J. Appl. Phys.* **1967**, *38*, 2535−2548.
(18) Pugh, S. F. *Philos. Mag.* **1954**, *45*, 823−843.